Proposal of a non-linear curve for reporting the performance of solar cookers

Celestino Rodrigues Ruivo[a,b,*], Xabier Apaolaza-Pagoaga[c], Gianluca Coccia[d], Antonio Carrillo-Andrés

[a] *Department of Mechanical Engineering, Institute of Engineering, University of Algarve, Campus da Penha, 8005-139 Faro, Portugal*

[b] *ADAI - LAETA, Rua Pedro Hispano nº12, 3030-289, Coimbra, Portugal*

[c] *Energy Research Group. Department of Mechanical, Thermal and Fluids Engineering, University of Malaga. Calle Arquitecto Francisco Peñalosa, 6, 29071, Malaga, Spain*

[d] *Marche Polytechnic University, Department of Industrial Engineering and Mathematical Sciences, Via Brecce Bianche 12, 60131 Ancona, Italy*

Abstract

Performance parameters of solar cookers have conventionally been determined by assuming a linear trend between the cooker power and the difference between load temperature and ambient air temperature. This approach may not be convenient for some solar cooker designs. In the present work, the suitability of a non-linear regression derived from fitting the measured load temperature to a second order exponential polynomial was investigated and compared with the linear regression. Both regressions were compared with the corresponding experimental curves of a panel cooker and a box cooker. In the case of the panel cooker, the linear trend of the experimental plot was confirmed over a large period of the conducted test. Minor deviations from the experimental data were

* Corresponding author; e-mail: cruivo@ualg.pt

observed only at the beginning and at the end of the test. On the contrary, in the box solar cooker, significant deviations between the linear regression plot and the experimental points were observed, while smaller deviations were obtained using the non-linear regression. Thus, the proposed method can be seen as a promising approach that should be considered when updating the existing procedures for testing and reporting the performance of solar cookers.

Keywords: solar cookers, experimental test; linear performance curve, non-linear performance curve, performance evaluation.

Nomenclature

A_n	Normal area to the sun rays being collected by the solar cooking device (m^2)
$A_{n,max}$	Maximum normal area to the sun rays being collected by the solar cooking device (m^2)
COR	Opto-thermal ratio of the solar cooking device (m^2 ºC W^{-1})
$c_{1,0}$	Parameter of the first order exponential polynomial of Eq. (8) (ºC)
$c_{1,1}$	Parameter of the first order exponential polynomial of Eq. (8) (ºC)
$c_{2,0}$	Parameter of the second order exponential polynomial of Eq. (22) (ºC)
$c_{2,1}$	Parameter of the second order exponential polynomial of Eq. (22) (ºC)
$c_{2,2}$	Parameter of the second order exponential polynomial of Eq. (22) (ºC)
I_n	Global solar irradiance in the plane perpendicular to the sun rays ($W\ m^{-2}$)
$\bar{I}_n$	Average value of the irradiance I_n during a test ($W\ m^{-2}$)
$\dot{Q}$	Power of the solar cooker (W)
$\dot{Q}_{in}$	Heat transfer rate associated with the solar radiation collected by the solar cooking device (W)

$\dot{Q}_{\text{in,id}}$	Heat transfer rate associated with the solar radiation collected by the solar cooking device being operated with perfect tracking (W)
T_{a}	Temperature of outdoor ambient air temperature (ºC)
$\bar{T}_{\text{a}}$	Average value of temperature T_{a} during a test (ºC)
T_{f}	Temperature of the load (ºC)
$T_{\text{f,0}}$	Initial temperature of the load (ºC)
t	Time (s)
t_1	Parameter of the first order exponential polynomial of Eq. (8) (s)
t_2	Parameter of the second order exponential polynomial of Eq. (22) (s)

Greek symbols

α_0	Parameter of the linear regression for the efficiency given by Eq. (5)
α_1	Parameter of the linear regression for the efficiency given by Eq. (5) (W ºC^{-1} m^{-2})
χ	Specific temperature difference, i.e., the ratio of ratio between $\Delta T_{\text{f,a}}$ and $\bar{I}_{\text{n}}$ (ºC m^2 W^{-1})
Δt_j	Time interval used in Eq. (35) (s)
$\Delta T_{\text{f,a}}$	Difference between the temperature of load being heated and the temperature of the outdoor ambient air (ºC)
η	Instantaneous efficiency associated with the heating of the load
Ω	Thermal capacitance of the load (J ºC^{-1})

1. Introduction

The performance evaluation of solar cooking systems has been investigated mainly by conducting experimental measurements, applying simplified analysis and testing procedures by researchers in different regions of the world, and in some cases also through numerical modelling. The literature dedicated to solar cookers is very large, thus a complete analysis is beyond the scope of the present study. In this work, however, we would like to focus our attention on recent papers that, in some extent, highlighted issues or the need for improved investigations when evaluating the thermal performance of solar cookers.

In 2007, Nandwani [1] designed a multi-purpose system (also referred to as hybrid food processor) evaluating various technical and practical aspects. The author assessed the performance of the system in Costa Rica according to different working modes: a) as a solar cooker; b) to pasteurize water; c) as a solar dryer; d) as a solar still. The cooker was able to combine solar and electric energy, using the minimum amount of the latter when required. For example, when used as a solar cooker, the system was tested using a stainless-steel pot and a thermal load including 600 g of meat with 550 g of potatoes, and 1006 g of cake mix (eggs, oil, water). Due to a change in weather conditions, at 11:00 am the cooker was also connected to electricity, setting a thermostat to 120-130 °C. Electricity was disconnected at 12:15 am, while cooking was stopped at 12:45 am; both meals were found to be properly cooked. The effective thermal efficiency of the multi-purpose system was found to be 23-32 %, depending on the working mode.

In 2013, Lecuona et al. [2] experimentally and numerically studied a portable parabolic solar cooker incorporating a daily thermal energy storage consisting of coaxial cylindric pots whose annulus was filled with paraffin and erythritol, used as phase change materials. The numerical analysis was carried out by means of a lumped elements model, able to identify the transient behaviour of the system. The model was validated with

94 experimental data collected in Madrid-Spain. Results indicated that it was possible to
95 cook three meals for a family, both in summertime and wintertime, using the proposed
96 thermal energy storage unit. Specifically, the authors highlighted that in wintertime the
97 thermal energy unit should be moved indoors for heat retention at least 2 hours earlier
98 than in summertime.
99 In 2017, Coccia et al. [3] constructed and tested a solar box cooker with a high
100 concentration ratio equal to 11.12. The authors conducted several tests using water,
101 peanut oil and no load. When water was used as thermal load, it was possible to boil 1 kg
102 of it in about 11 min, and this time could be further reduced when two pots were loaded
103 in the solar box cooker. When, instead, peanut oil was tested, temperatures higher than
104 200 °C were achieved, proving that the solar box cooker was able to cook food fast and
105 at high temperatures.
106 In 2018, Collares-Pereira et al. [4] listed that numerous testing procedures and figures of
107 merit have been proposed to evaluate the performance of solar cookers. For instance, in
108 India a standard procedure has been proposed by the Bureau of Indian Standards, but it
109 presents limitations that can be eliminated only by studying in more detail the thermal
110 behaviour of solar cookers. For this reason, the authors proposed a revision of the
111 procedure and found that the results obtained with the new proposal are more adherent to
112 experimental data. Also, they were able to model the behaviour of a solar cooker at
113 different times of the year.
114 Edmonds [5] proposed a low-cost solar cooker with a non-imaging concentrator including
115 eight flat reflective panels. The cooker was experimentally evaluated both with low and
116 high temperature cooking, where the latter was possible by modifying the base of the
117 cooking pan with a solar selective material or a transparent glazing. According to the
118 experimental results obtained by the author, the proposed design was able to reach

temperatures higher than 260 °C during clear-sky conditions. The author also highlighted that no detailed testing procedures and figures of merit were assessed as that was the first proposal for that kind of solar cooker design.

In 2018, Sagade et al. [6] proposed a procedure to identify the most suitable tests for selecting various designs of solar cookers at intermediate temperature (120–240 °C), which are considered interesting due to their wide range of cooking possibilities. The authors considered two working fluids (water and glycerine) and two designs of solar cooker (box solar cooker and square parabolic dish solar cooker). The cooker opto-thermal ratio (*COR*) was used as performance indicator. The results of the analysis indicated that the proposed procedure yielded approximately identical values of the *COR* for a specified design, thus enabling its rating at intermediate temperatures. It was also seen that a change in the design had a large impact on the *COR*, but this was not confirmed for the solar box cooker.

In 2020, Ebersviller et al. [7] adopted the ASAE (American Society of Agricultural Engineers) Standard S580.1 (Testing and Reporting Solar Cooker Performance) [8] to evaluate the thermal performance of household solar cookers. Specifically, the authors tested a parabolic cooker, a box cooker and a panel cooker, analysing in detail the issues correlated to water evaporation. It was found that the energy used for water evaporation is less than the energy used for heating water, but nevertheless it represents a fraction not considered in the calculation of the cooking power as defined in the ASAE S580.1. The maximum amount of evaporated water was found for the solar panel cooker; at low temperatures, calculated cooking power is accurate because only a negligible amount of water evaporates, but at high temperatures the calculation is less accurate. According to the authors, the bias may be eliminated by ending the test 20 °C below the boiling temperature, but in this case the regression line of the cooking power should be

extrapolated up to a temperature difference of 50 °C, since ASAE S580.1 requires evaluation of the cooking power at that temperature difference. The authors suggested other solutions to overcome the problem related to water evaporation, however each of them is associated with other drawbacks. For this reason, the authors concluded their analysis suggesting the need for additional experimental tests, in order to identify the best approach to eliminate the bias.

Khallaf et al. [9] proposed in 2020 a new design of solar cooker referred to as Quonset. The cooker consists of a dome-shaped transparent cover made of fiberglass reinforced plastic and twin cooking compartments. The performance of the cooker was evaluated experimentally at low and intermediate temperatures. The authors also provided a mathematical model to assess the thermal performance of the cooker and to carry out a comparison between experimental and numerical results. Numerous parameters were considered by the authors in the analysis (cooking power, cooker efficiency, *COR*). In particular, it was found that the cooking power evaluated at a temperature difference of 50 °C, using either water or glycerine, was higher than that obtained for good designs of solar box cookers. According to the authors, this and the other results proved that the proposed design can be used to cook many items at low and intermediate temperatures.

Sagade et al. [10] evaluated the use of a modified cooking pot in a solar box cooker, in order to assess the performance improvement due to the adoption of a novel cooking vessel. The authors used *COR* as thermal performance parameter and carried out outdoor tests comparing the proposed pot with a conventional cooking pot. The authors found relevant improvements with the new pot design, due to the effective thermal barrier provided by the glass lid. It was also highlighted that the proposed testing procedure succeeded in quantifying in an unambiguous way the improvement in the cooker performance.

In 2021, Tawkif et al. [11] discussed a new design of solar cooker equipped with internal reflectors and a tracking-type bottom parabolic reflector. The thermal performance of the cooker was evaluated using glycerine as the thermal load. *COR* and many other testing parameters were evaluated by the authors. Results showed that the *COR* was equal to 0.123 (m^2 °C)/W when the parabolic reflector was not used, and 0.165 (m^2 °C)/W when it was installed in the system. Based on the evaluations of the authors, the cooker should be considered suitable for temperatures of 140 – 150 °C.

Ruivo et al. [12] analysed the performance of a funnel solar cooker using, whenever possible, the ASAE S580.1 Standard. Some additional procedures were considered to improve the protocols of the Standard. The authors carried out experimental tests with care, using a specific methodology; measurements were taken in Malaga, Spain, between November 2019 and February 2020, a period characterized by sun at low elevation. The influence of two different lids was assessed by evaluating the corresponding cooking power. Results indicated that, using a glass lid, the standardized cooking power was 73.9 W, while using a black metal lid a value of 50.6 W was determined. In their analysis, the authors also suggested that the ASAE S580.1 Standard should be updated to take into account the existing differences between the available types of solar cookers, cooking set characteristics, and broader ranges of weather conditions. For instance, the authors suggested that the ratio between water load and reflector area recommended for funnel cookers is not suitable. In addition, the standardized cooking power evaluated at a temperature difference of 50 °C should be revised, because this temperature often occurs during the heating process in many applications, before the actual cooking of food.

Continuing their analysis on funnel cookers, Apaolaza-Pagoaga et al. [13] investigated their applicability for temperatures higher than the boiling point of water. The authors tested two identical funnel cookers; one cooker had a glass enclosure, while the other one

had no enclosure. Different parameters were considered to evaluate the performance of the cookers, including *COR* and overall cooker efficiency. Results showed that the use of the glass enclosure enabled temperatures of 140 – 150 °C to be reached; using glycerine as test load, *COR* for the two funnel cookers was found to be 0.110 (m^2 °C)/W for the device without a glass enclosure, and 0.157 (m^2 °C)/W for the device with glass enclosure. The corresponding efficiencies were evaluated at 10.2 % and 11.8 %, respectively.

In a following paper, Apaolaza-Pagoaga et al. [14] determined the cooking powers of two funnel cookers using the ASAE S580.1 Standard. The authors also proposed a new approach to evaluate in more detail the effect of minor changes in the design of the cookers. It was found that the variation in the cooking power due to small modifications is low, but not negligible; e.g., the cooking power increased by 6 W when a 25-mm trivet was used. Based on the opinion of the authors, the proposed approach is useful because it is not performable with the ASAE S580.1 Standard.

The analysis of the literature, even if partial, reveals that different test parameters and procedures have been used by researchers during recent years. This compromises the possibility of carrying out comparisons. Also, several authors highlighted the need to revise and improve the ASAE S580.1 Standard [8], which is generally adopted when testing solar cookers. The Standard, in fact, reports a well-known procedure to test and report the performance of the most common solar cooker designs that is based on the linear dependence of the cooking power on the difference between load temperature and ambient air temperature, obtained by using experimental data from the cooker. As can be seen from the previous literature review, another procedure generally considered to estimate cooker characteristic parameters is the cooker opto-thermal ratio (*COR*), as proposed by Lahkar et al. [15]. The procedure to determine *COR* is also based on a linear

regression performance curve using instantaneous efficiency instead of cooker power and using water as load.

1.1 Linear regression for evaluating the performance parameters of a solar cooker

In a recent paper, Ruivo et al. [16] found that the procedures based on the linear regression performance curve, derived from experimental testing data, may produce unrealistic values for the performance parameters of some solar cooker designs as is the particular case of the box solar cooker design tested by Coccia et al. [3]. They may be associated with the non-negligible thermal inertia of components of the cooking chamber.

The plots of the efficiency for the funnel cooker design tested with glycerine [16] also shows that the power increased from the beginning of the experiment, but only during a relatively short period. This phenomenon is not observed in the plots of the analysis carried out by Funk [17], who showed that the linear regressions of tests with a water load ratio of 7 kg m^{-2} agree well with the experimental measured data and the use of a more accurate regression does not produce substantial improvements. The phenomenon may be justified by the fact that the testing data used by Ruivo et al. [16] applies to cases with significantly lower load ratio values, because the box solar cooker was tested with a peanut oil load ratio of 1.68 kg m^{-2} and the funnel solar cooker was tested with a glycerine load ratio of 3.47 kg m^{-2}. It is important to point out that the observation points registered at the end of each test presented by Funk [17] evidence a non-negligible deviation between experimental values and the linear trend. A similar deviation was observed by Ruivo et al. [16] at the end of the test of a funnel cooker loaded with glycerine, in this case due mainly to a loss of optical efficiency at the end of the test that resulted from a significant increase of the angle of incidence during this part of the test. The optical efficiency would be almost constant if the test were conducted with perfect tracking in both axes. Thus, most probably the non-negligible deviation mentioned previously in the

243 plots of Funk [17] can be attributed to the loss of optical efficiency of the box solar cooker
244 tested with water.
245 The majority of the reports of tested solar cookers show that the linear regression
246 expressing the relationship between the cooker power and the temperature difference
247 between load and ambient has a negative slope [12,17,18,19], but the determined linear
248 regression shown in some reports has an opposite trend as in the case of the GoSun Sizzle
249 cooker [19] and the box solar cooker tested by Sethi et al. [20]. The same positive slope
250 would be observed if the peanut oil test ended at a load temperature of 95 ºC with the box
251 solar cooker of Coccia et al. [3]. The tests carried out by Coccia et al. [3] using water and
252 glycerine as loads are clear examples of the non-suitability of the derived linear regression
253 performance curve because the use of a linear regression performance curve with a
254 positive slope does not make any sense when estimating cooker characteristic parameters
255 such as the cooker opto-thermal ratio introduced by Lahkar et al. [15]. Coccia et al. [3]
256 overcame this problem by disregarding test data from the initial period where load
257 temperature was less than 60 ºC.
258 Data from experiments conducted with a panel solar cooker and a box solar cooker, used
259 in a previous research paper [16] and adopting glycerine and peanut oil as loads,
260 respectively, were again selected to investigate the suitability of a new approach for
261 evaluating the thermal performance of different solar cooker designs. The new approach
262 is based on a second order exponential polynomial to fit the experimental plot of the load
263 temperature during a test. The derived efficiency curve was compared with the same
264 curve determined by using a simpler approach based on the first order exponential
265 polynomial and also with the performance curve estimated directly from experimental
266 data without performing any fitting procedure.

1.2. Impact of cooking vessel and solar cooking chamber components on the cooker performance curve

The performance of a solar cooker is strongly influenced by the cooking vessel and cooker components that vary strongly according to the type of cooker. Regarding the cooking vessel, the performance of any type of solar cooker depends on the thickness, weight and properties of the materials used for the cooking vessel.

In the case of a box solar cooker, mass, thickness and properties of each layer of material used in the opaque and transparent parts of the envelop have an important impact on its performance as well as the use of eventual dedicated thermal storage elements used in the cooking chamber of this type of cooker.

The type of heat trap device usually adopted in panel cookers also has an important influence on the performance of the cooker. Plastic bags or polycarbonate enclosures have been chosen to act as greenhouse devices in some panel cooker designs [21–23], which have low thermal inertia and low thermal resistance to the heat transfer being lost from the pot to the surrounding environment. Thus, the thermal inertia of a panel cooker operating in these circumstances is mainly associated with the load. The same happens with the performance of common parabolic dish solar cookers when the user is cooking with a non-massive pot. If a massive and thick pot is used in any type of cooker, its average temperature and load temperature are expected to grow at different rates. The same is expected to happen with the cooking chamber elements of non-negligible mass for a box solar cooker and when a massive glass enclosure is used as a heat trap in a panel solar cooker or even in a parabolic solar cooker to guarantee that food is well cooked under cold wind or intermittent cloudy conditions. When using special dedicated media for storing thermal energy, in sensible or in both sensible and latent forms, the evolution of the load temperature will strongly depend on whether the cooking chamber is pre-

heated or not before conducting the test with the load. Some of these issues have been addressed in few studies, but not with the purpose of investigating the validity of using the linear regression performance curve. The linear regression performance curve was used to determine the opto-thermal ratio values for a funnel solar cooker with and without a massive glass enclosure [13], a box solar cooker with a glass or metal lid on the black metal pot [10], and for parabolic and box solar cookers with non-coated pots and with matt black coated pots [6]. In other studies, the linear regression performance curve was used to determine the standardised power for a funnel solar cooker with a massive glass enclosure and with a glass or metal lid on the black metal pot [12], and for a box cooker using an absorber plate with one or four pots [24].

1.3 Aim of present study

A relatively high number of studies about testing and reporting the performance of solar cooker have been done and the respective data are available in the scientific literature. Some of the conducted studies were based on the linear regression performance curve. To the authors' knowledge, the investigation of an approach based on a better regression performance curve has not yet been conducted. Thus, following the previous work of Ruivo et al. [16] and using the same experimental data derived from a box solar cooker and a panel solar cooker, the present work aims to: i) provide insights about the weakness of the linear regression when applied to some solar cooker designs, and ii) present a non-linear performance curve that is capable of overcoming some of the limitations of the linear regression curve.

2. Simplified evaluation of the performance of a solar cooker

The detailed analysis of the coupled and transient heat and mass transfer phenomena taking place in a solar cooker during the load heating process is too complex to be solved analytically. The lumped capacitance thermal model is usually adopted to simplify the

317 analysis, i.e., the temperature of the system, T_f, is considered uniform and it varies during
318 the heating process. In the present work, the load is assumed to be the system, which
319 receives thermal energy at a rate $\dot{Q}$. This rate is the useful power of the cooker, which
320 corresponds to the rate of variation of thermal energy stored in the load:

321 $$\dot{Q} = \Omega \frac{dT_f}{dt} \quad (1)$$

322 where Ω is the thermal capacitance given by the product of the mass and specific heat of
323 the load.

324 The power $\dot{Q}$ is expected to vary during the load heating test due to the changes in the
325 rate of absorbed thermal radiation by the pot containing the load and in the rate of the
326 thermal losses from the pot to its surroundings. It is important to point out that a fraction
327 of the solar energy being collected by the reflectors is also used to heat up the pot and
328 other components such as the glass enclosure used as heat trap in case of panel cookers
329 or the materials of the envelop of a cooking chamber in the case of box cookers, and part
330 of that energy is lost to the surroundings by convection, conduction and radiation.
331 Moreover, there are also some thermal losses associated with the ventilation, intended or
332 not, of the cooking chamber of a box cooker or the cooking chamber formed by the heat
333 trap in the case of a panel cooker. Energy losses due to evaporation can also occur, when
334 using water as a load.

335 The energy transfer rate associated with the solar radiation intercepted by the cooker at
336 any instant is given by:

337 $$\dot{Q}_{in} = I_n A_n \quad (2)$$

338 where A_n and I_n represent the normal area to the incoming beam solar radiation being
339 collected by the solar cooker and the normal solar irradiance, respectively. When the
340 cooker is operating without perfect sun tracking, the area A_n varies. In these

341 circumstances, the area A_n becomes smaller than its maximum value $A_{n,max}$. Thus, in
342 the case of perfect sun tracking, the ideal energy transfer rate would be evaluated as:

343 $$\dot{Q}_{in,id} = A_{n,max} I_n \quad (3)$$

344 By considering this ideal input rate of solar energy into the cooker system, the
345 instantaneous efficiency of the load heating process can be expressed by the following
346 ratio:

347 $$\eta = \frac{\dot{Q}}{A_{n,max} I_n} \quad (4)$$

348 According to this definition, the efficiency also takes into account the degradation of the
349 efficiency associated with the imperfect tracking of the cooker.

350 **2.1 Performance evaluation based on a first order exponential polynomial**

351 The linear regression usually adopted to derive a relationship between the load and the
352 outdoor air temperature difference $\Delta T_{f,a}$ and the power can be presented alternatively in
353 terms of instantaneous efficiency:

354 $$\eta = \alpha_0 - \alpha_1 \chi \quad (5)$$

355 where the variable χ represents the specific temperature difference, which is defined by
356 the ratio between $\Delta T_{f,a}$ and I_n [23]:

357 $$\chi = \frac{T_{f,a} - T_a}{I_n} \quad (6)$$

358 In the context of the present work, it is assumed in the calculations of both η and χ
359 variables that the solar irradiance I_n during a test is constant and equal to the respective
360 average value $\bar{I}_n$. The same applies to ambient temperature when calculating χ. This
361 means that the present approach is limited only for cases of tests where variations of solar

362 irradiance and ambient temperature are relatively small. Thus, the linear regression
363 expressed by Eq. (5) can also be written by:

364 $$\frac{dT_{\mathrm{f}}}{dt} = \frac{A_{\mathrm{n,max}}\bar{I}_{\mathrm{n}}}{\Omega}\left(\alpha_0 - \alpha_1\chi\right) \tag{7}$$

365 It means that a first order exponential polynomial can represents the dependence of the
366 load temperature on the evolution time of the process written in the following form:

367 $$T_{\mathrm{f}} = c_{1,1}\exp\left(-\frac{t}{t_1}\right) + c_{1,0} \tag{8}$$

368 The corresponding inverse function is

369 $$t = t_1 \ln\left(\frac{c_{1,1}}{T_{\mathrm{f}} - c_{1,0}}\right) \tag{9}$$

370 The constants $c_{1,0}$, $c_{1,1}$ and t_1 can be determined by a curve fitting process of the
371 experimentally measured temperature.

372 Applying the definition given by Eq. (1), the efficiency given by Eq. (4) can be predicted
373 as a function of time by:

374 $$\eta = \frac{-\Omega c_{1,1}}{t_1}\exp\left(-\frac{t}{t_1}\right)\frac{1}{A_{\mathrm{n,max}}\bar{I}_{\mathrm{n}}} \tag{10}$$

375 or as a function of χ by using the following expression:

376 $$\eta = \frac{\Omega}{A_{\mathrm{n,max}}\bar{I}_{\mathrm{n}}}\frac{c_{1,0} - \bar{T}_{\mathrm{a}}}{t_1} - \frac{\Omega}{A_{\mathrm{n,max}}t_1}\chi \tag{11}$$

377 Thus, the coefficients of the linear regression expressed by Eq. (5) are given by:

378 $$\alpha_0 = \frac{\Omega}{A_{\mathrm{n,max}}\bar{I}_{\mathrm{n}}}\frac{c_{1,0} - \bar{T}_{\mathrm{a}}}{t_1} \tag{12}$$

379 $$\alpha_1 = \frac{\Omega}{A_{\mathrm{n,max}}t_1} \tag{13}$$

Considering $T_{f,0}$ as the temperature of the load at the initial instant, i.e. at $t = 0$, it follows from Eq. (7) that:

$$c_{1,1} + c_{1,0} = T_{f,0} \tag{14}$$

By using the relationships expressed by Eqs. (12) to (14), it is possible to demonstrate that Eq. (8) can also be written in the following form:

$$T_f = \left(T_{f,0} - \overline{T}_a - \frac{\alpha_0 \overline{I}_n}{\alpha_1} \right) \exp\left(-\frac{\alpha_1 A_{n,max}}{\Omega} t \right) + \overline{T}_a + \frac{\alpha_0 \overline{I}_n}{\alpha_1} \tag{15}$$

This result shows that the parameters $c_{1,1}$, $c_{1,0}$ and t_1 can be estimated from the linear regression obtained from plotting the experimental results of one test in terms of η versus χ. Moreover, the time needed for the load to achieve a certain temperature that corresponds to a particular value of χ can be estimated by:

$$t = \frac{\Omega}{\alpha_1 A_{n,max}} \ln\left(\frac{\frac{T_{f,0} - \overline{T}_a}{\overline{I}_n} - \frac{\alpha_0}{\alpha_1}}{\chi - \frac{\alpha_0}{\alpha_1}} \right) \tag{16}$$

From Eqs. (15) and (16), parameter t_1 corresponds to:

$$t_1 = \frac{\Omega}{\alpha_1 A_{n,max}} \tag{17}$$

The approach based on fitting experimental measured data with Eq. (8) and the corresponding linear regression expressed by Eq. (11) was adopted in some previous studies [3,11,13] to determine the cooker opto-thermal ratio. This ratio corresponds to the value of the abscissa of point H1, a point that is defined by the intersection of the linear regression expressed by Eq. (5) and the horizontal axis. It can be estimated by:

$$COR = \chi_{H1} = \frac{\alpha_0}{\alpha_1} \tag{18}$$

Using Eqs. (12) and (13), the same cooker parameter can be determined by:

$$COR = \chi_{\mathrm{H1}} = \frac{c_{1,0} - \bar{T}_{\mathrm{a}}}{\bar{I}_{\mathrm{n}}} \tag{19}$$

The point V1 defined by the intersection of the linear regression, expressed by Eq. (5), with the vertical axis, corresponds to the point of maximum efficiency when the cooker performance curve is linear. At this point the efficiency η_{V1} is equal to α_0.

The approach based on fitting experimental measured data with Eq. (8) and the corresponding linear regression expressed by Eq. (11) does not correspond exactly to the approach recommended by the standard [8]. It is here used for predicting the cooker efficiency for $\Delta T_{\mathrm{f,a}} = 50\,^{\circ}\mathrm{C}$, reference point R1, as:

$$\eta_{\mathrm{R1}} = \frac{\Omega}{A_{\mathrm{n,max}} \bar{I}_{\mathrm{n}}} \frac{c_{1,0} - 50}{t_1} \tag{20}$$

or in terms of the cooker opto-thermal ratio as:

$$\eta_{\mathrm{R1}} = \frac{\Omega}{A_{\mathrm{n,max}} t_{\mathrm{ref}}} \left(COR - \frac{50}{\bar{I}_{\mathrm{n}}} \right) \tag{21}$$

2.2 Performance evaluation based on a second order exponential polynomial

As mentioned before, the plots presented by Coccia et al. [3] clearly indicate that the linear regression is not applicable to all solar cooker designs. Thus, a more accurate regression is needed to perform the evaluation of a solar cooker design. The new regression is based on the following second order exponential polynomial that fits the time evolution of the fluid temperature during the load heating process:

$$T_{\mathrm{f}} = c_{2,2} \left(\exp\left(-\frac{t}{t_2} \right) \right)^2 + c_{2,1} \exp\left(-\frac{t}{t_2} \right) + c_{2,0} \tag{22}$$

The values of the constants $c_{2,2}$, $c_{2,1}$, $c_{2,0}$ and t_2 can be also determined through a curve fitting process of the experimentally measured temperature. From Eq. (22), it can be proved that:

421 $$\exp\left(-\frac{t}{t_2}\right)=\frac{-c_{2,1}-\sqrt{c_{2,1}^2-4c_{2,2}\left(c_{2,0}-T_{\mathrm{f}}\right)}}{2c_{2,2}} \tag{23}$$

422 This allows a prediction of the time period as a function of temperature:

423 $$t=-t_2\ln\left(\frac{-c_{2,1}-\sqrt{c_{2,1}^2-4c_{2,2}\left(c_{2,0}-T_{\mathrm{f}}\right)}}{2c_{2,2}}\right) \tag{24}$$

424 Applying the definitions of power and efficiency given by Eqs. (1) and (4), respectively,
425 the efficiency can be predicted as a function of time by:

426 $$\eta=\left(-\frac{2\Omega c_{2,2}}{t_2}\left(\exp\left(-\frac{t}{t_2}\right)\right)^2-\frac{\Omega c_{2,1}}{t_2}\exp\left(-\frac{t}{t_2}\right)\right)\frac{1}{A_{\mathrm{n,max}}\bar{I}_{\mathrm{n}}} \tag{25}$$

427 or as a function of χ by using the following expression:

428 $$\eta=\frac{-\Omega\left(c_{2,1}\sqrt{c_{2,1}^2-4c_{2,2}\left(c_{2,0}-\chi\bar{I}_{\mathrm{n}}-\bar{T}_{\mathrm{a}}\right)}+c_{2,1}^2-4c_{2,2}\left(c_{2,0}-\chi\bar{I}_{\mathrm{n}}-\bar{T}_{\mathrm{a}}\right)\right)}{2c_{2,2}t_2A_{\mathrm{n,max}}\bar{I}_{\mathrm{n}}}$$

429 (26)

430 Fig. 1 depicts the performance curves of a solar cooker, in terms of η versus χ. Fig. 1a)
431 illustrates the performance curve of a cooker showing an initial period where the
432 efficiency achieves its maximum at a certain time after starting the test, an intermediate
433 period evidencing a linear decreasing of the efficiency and a final period where the load
434 is approaching the stagnation stage. The initial period corresponds to the initial warming
435 up transient period where the stored thermal energy rate of the components of the cooking
436 chamber is higher than the rate of energy being transferred to the load. Thus, the duration
437 of this initial period is expected to be small in most solar cooker designs where load
438 thermal capacitance is much higher than the values of the thermal capacitance of the
439 cooking vessel and other components of the cooking chamber. The intermediate period is

expected to be observed in most solar cooker designs when the optical efficiency and the solar irradiance do not change significantly during the cooker test.

In Fig 1b), curve 1 corresponds to the linear regression derived from the first order exponential polynomial and curve 2 corresponds to the regression derived from the second order polynomial. When using curve 1, its intercept on the vertical axis (point V1), and its intercept on the horizontal axis (point H1) are sufficient to define the respective straight line. In the case of curve 2 defined by Eq. (26), its intercept on the vertical axis (point V2) and its intercept on the horizontal axis (point H2) are not enough to define the curve. Another important point on this curve is point C2, at which the power is maximum. In the same Fig. 1, the point R1 on curve 1 represents the reference point adopted by the Standard to report the power for $\Delta T_{\mathrm{f,a}} = 50\,^{\circ}\mathrm{C}$, i.e., $\chi = 50 / \bar{I}_{\mathrm{n}}$. The point R2 for curve 2 has the same meaning but is adapted to the new approach.

The parameter COR given by Eq. (17) corresponds exactly, in curve 1, to the χ coordinate of the point H1 ($\chi = \chi_{\mathrm{H1}}$). Thus, the COR value of a solar cooker design exhibiting a performance curve similar to curve 2 is overestimated when using the data from curve 1.

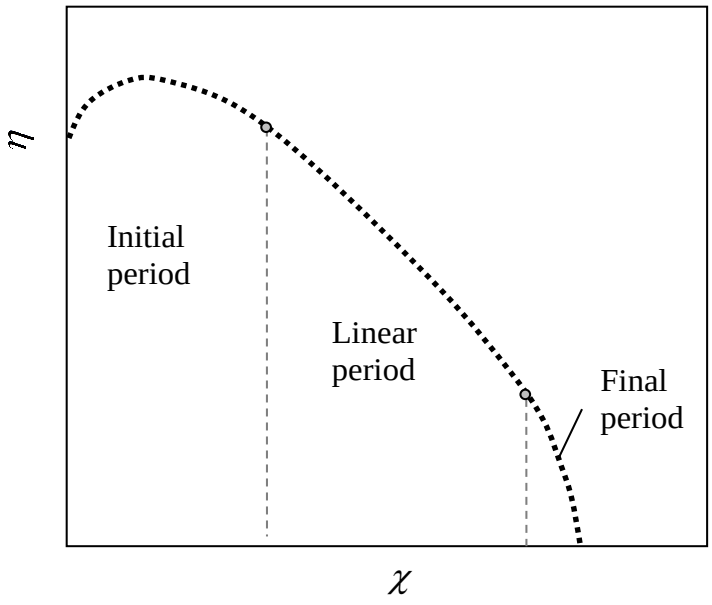

456 a)

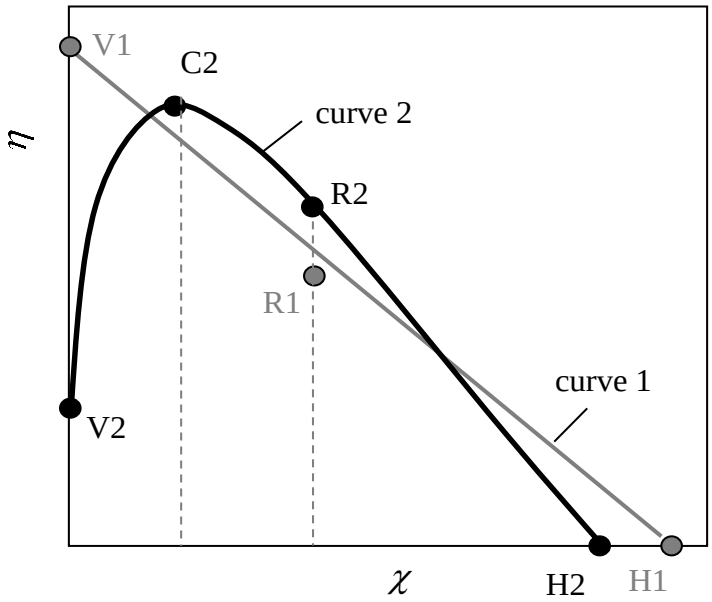

457

458 b)

459 Fig. 1. Schematic representation of the two performance curves: linear regression (curve
460 1) and non-linear regression (curve 2).

461 It can be demonstrated that, for the point C2, the efficiency and the specific temperature
462 difference are given, respectively, by:

463 $$\chi_{C2} = \frac{c_{2,0} - \frac{3c_{2,1}^2}{16c_{2,2}} - \bar{T}_a}{\bar{I}_n} \tag{27}$$

464 $$\eta = \frac{\Omega c_{2,1}^2}{8c_{2,2}t_2 A_{n,max}\bar{I}_n} \tag{28}$$

465 For the point V2, the values of the same variables are given by the following expressions:

466 $$\chi_{V2} = \frac{c_{2,2} + c_{2,1} + c_{2,0} - \bar{T}_a}{\bar{I}_n} \tag{29}$$

467 $$\eta_{V2} = -\frac{\Omega}{t_2}\frac{1}{\bar{I}_n A_{n,max}}\left(2c_{2,2} + c_{2,1}\right) \tag{30}$$

The coordinate χ_{V2} of the point V2 is strictly equal to zero only when $T_{f,0} = \overline{T}_a$.

For the point H2, the values of the same variables are given by the following expressions:

$$\chi_{H2} = \frac{c_{2,0} - \overline{T}_a}{\overline{I}_n} \tag{31}$$

$$\eta_{H2} = 0 \tag{32}$$

The coordinate χ_{H2} of the point H2 can be seen as the cooker opto-thermal ratio estimated from curve 2, which is expected to be more accurate than the value derived from curve 1.

For the point R2, the values of the same variables are given by the following expressions:

$$\chi_{R2} = \frac{50}{\overline{I}_n} \tag{33}$$

$$\eta_{R2} = \frac{-\Omega\left(c_{2,1}\sqrt{c_{2,1}^2 - 4c_{2,2}\left(c_{2,0} - 50 - \overline{T}_a\right)} + c_{2,1}^2 - 4c_{2,2}\left(c_{2,0} - 50 - \overline{T}_a\right)\right)}{2c_{2,2}t_2 A_{n,max}\overline{I}_n} \tag{34}$$

2.3 Performance evaluation using the experimental measured data directly

Eq. (1) represents the rate of variation of sensible heat stored in the load. The derivative used to determine the rate of variation of the load temperature can be estimated directly from the measured load temperature during its heating process by a finite difference approach. Thus, the efficiency can be estimated as:

$$\eta = \Omega \frac{T_{f,j}^{f,exp} - T_{f,j}^{i,exp}}{\Delta t_j} \frac{1}{A_{n,max}\overline{I}_n} \tag{35}$$

where $T_{f,j}^{i,exp}$ and $T_{f,j}^{f,exp}$ are the temperature measured values at the initial instant and final instant of the time step Δt_j, respectively. The time step Δt_j recommended by the standard has a duration of 600 s [8], which may be questionable value when the thermal capacitance of the load and of other components is small. In such cases, a smaller time

step is recommended, being the minimum acceptable value dictated by the uncertainty associated with the measurements of the load temperature.

3. Analysis of the performance of two different designs of solar cooker

This section provides a brief description of the two solar cookers investigated (a panel and a box cooker), along with a detailed analysis of the experimental results and their discussion.

3.1 Brief description of the experimental setups and experimental data associated with tests of panel and box cookers

The present research is an extension of a recent published work [16]. Thus, the same set of experimental results was selected to support the present research, i.e., the experimental measured data of tests conducted in a panel cooker and in a box cooker, both with funnel-shaped reflectors as shown in Fig. 2 and 3.

Glycerine and peanut oil were used as loads when testing, respectively, the panel cooker on 11.11.2020 in the experimental setup located on the roof of a building at the University of Malaga - Spain and the box cooker on 01.07.2016 on the roof of a building at the Marche Polytechnic University - Italy.

a)

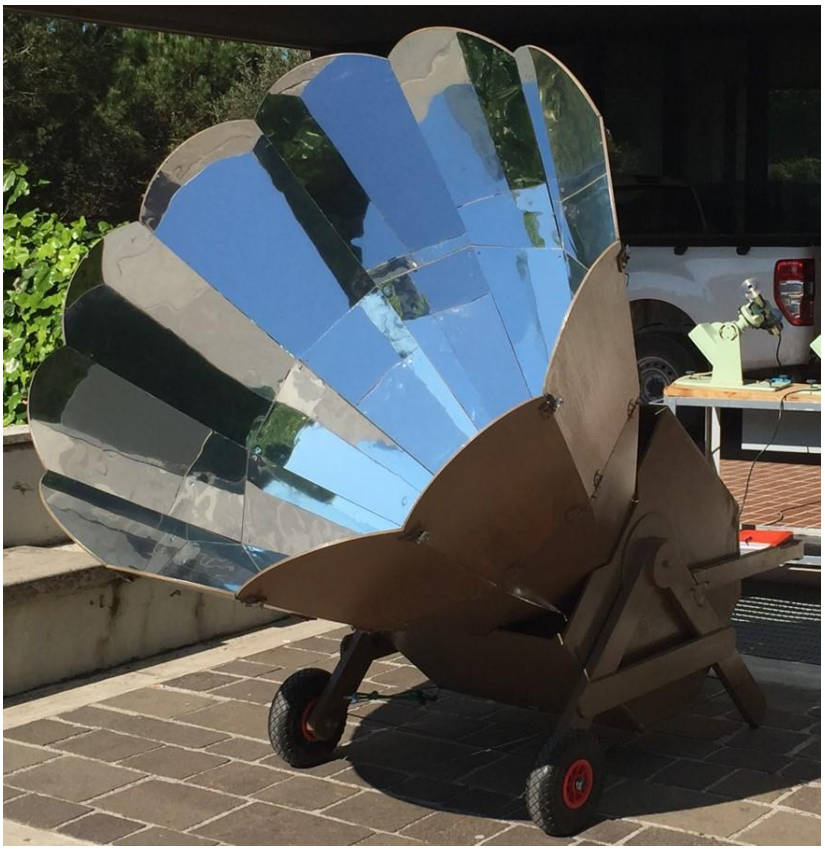

b)

Fig. 2. Designs of solar cookers with funnel-shaped reflectors used for the present investigation: a) panel cooker and b) box cooker.

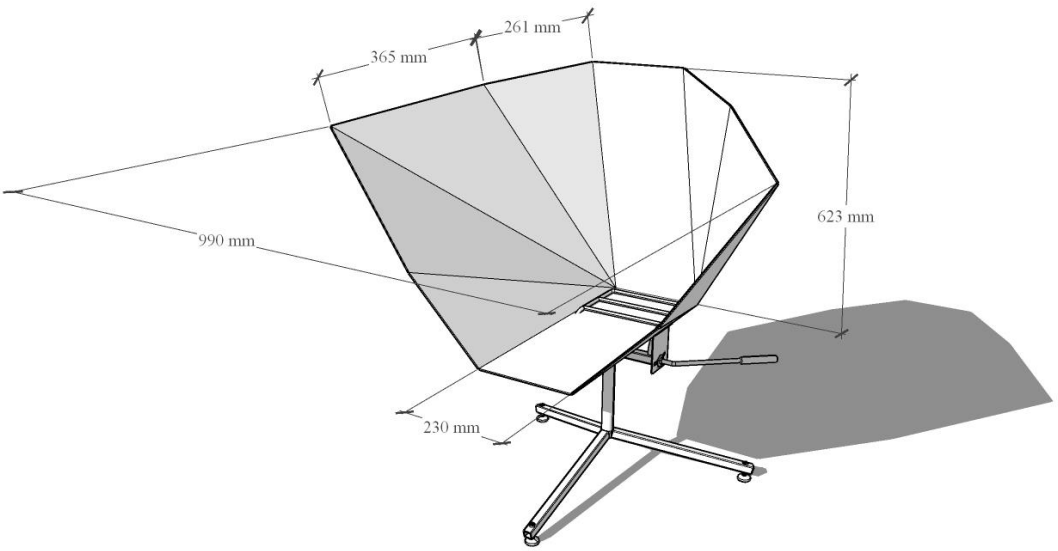

a)

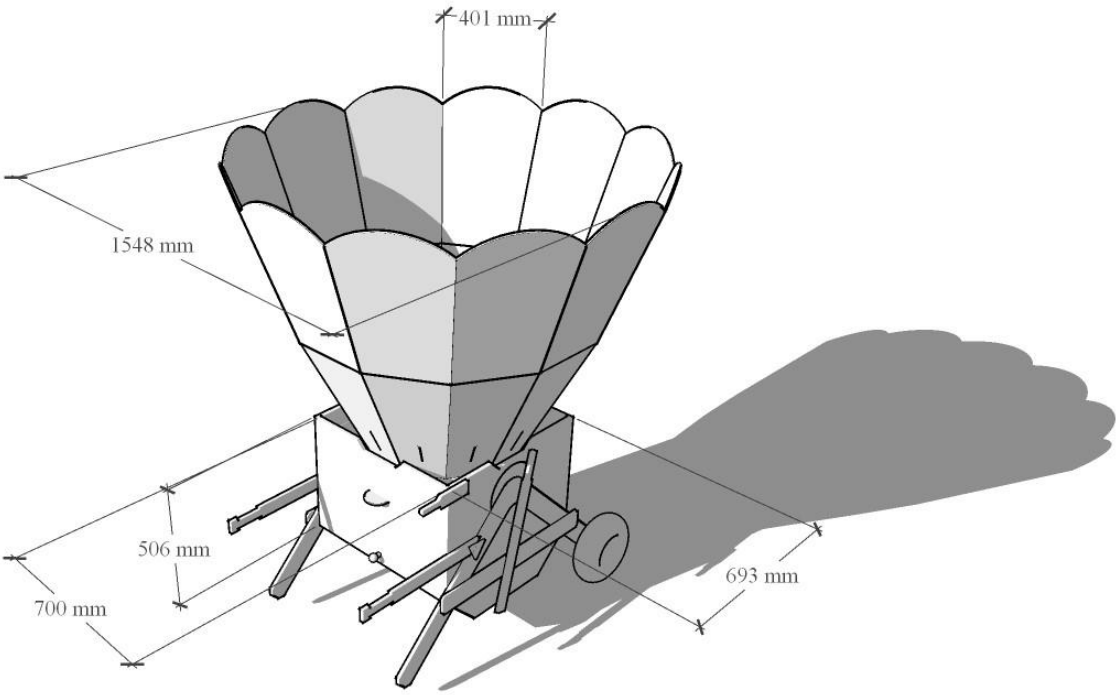

b)

Fig. 3. 3D schematics of the: a) panel cooker and b) box cooker.

Figs. 2a) and 3a) depict the reflector of the panel cooker, which is made of rectangles and triangles with polished aluminium surfaces. The maximum area of the panel cooker perpendicular to the incoming solar beam irradiation is 0.5 m^2, a value that is obtained only when testing the cooker with perfect tracking. The cooking set includes a massive glass enclosure. It is placed directly in the cooking zone, i.e., in direct contact with the horizontal rectangular reflector and close to the tilted rectangular reflector. The pot with a maximum capacity of 3 litres is made of black enamelled carbon steel. The mass values of the glass lid and pot are, respectively, 366 grams and 560 grams. The clear and thick glass enclosure weighs 2240 grams and was made of two re-used windows from discarded washing machine. The glass enclosure promotes the greenhouse effect around the pot. The results of the test here considered apply to a load of 1736 grams of glycerine occupying about half the capacity of the pot, and with the cooker tracked only

azimuthally. As mentioned in Ruivo et al. [16], the values of global solar irradiance were registered by two pyranometers placed close to the tested cooker, one on a tilted plane and the other on the horizontal plane. Moreover, global and diffuse solar irradiance values were also measured in the horizontal plane by the pyranometers of a meteorological station located on top of the same building. The beam and global normal irradiance values were estimated by the sky model of Liu-Jordan [25].

A dedicated Onset weather station was used for measuring the ambient temperature and wind speed. Five thermocouples were used to measure the glycerine temperature in different points, being the average temperature considered representative of whole body of glycerine and adopted in the calculations of the cooker power by using the exponential fitting or directly using the average experimental measured values. During the selected test, the tilted pyranometer was azimuthally adjusted at the same time of azimuth adjustment of the cooker, every 20 min.

Figs. 2b) and 3b) depict the box solar cooker. The box is a cooking chamber having a highly thermally insulated opaque envelop with a glass cover on its top. The reflection of the sun rays into the cooking chamber is performed by a multiple set of reflectors having a funnel shape. This cooker, when operating with a perfect alignment, has a maximum normal area to the incoming solar beam irradiation equal to 1.89 m^2. The geometric concentration ratio of this particular design of solar cooker is 11.12, a value more similar to the concentration ratio of common parabolic cookers than the value of common box cookers. The results of the selected test here considered apply to a load of 3 kg of peanut oil inside a cooking vessel weighing 135 g [3]. The temperature of the peanut oil and the outdoor ambient temperature were measured by means of thermocouples. During the test, the box cooker was adjusted each 300 s to guarantee an almost perfect reflector sun tracking. Coccia et al. [3] did not measure the global solar irradiance in the plane normal

552 to the sun's rays, but direct normal irradiance only. This choice was due to the fact that
553 the considered solar box cooker has a high concentration ratio (11.12), thus it is not able
554 to exploit diffuse radiation profitably. However, the measured direct normal irradiance
555 reported in [3] was not correct due to a wrong calibration curve of the pyrheliometer used.
556 A corrigendum of all measurements related to solar radiation has been published recently
557 [26]; the correct average normal direct solar irradiance of the test here considered from
558 [3] is equal to 810.8 W m^{-2}. Since in the experiments carried out by Ruivo et al. [12] for
559 17 days the global normal solar irradiance was, on average, 11% higher than the direct
560 normal irradiance, in the present work a 10% greater average solar radiation was assumed.
561 Therefore, the average global normal solar irradiance during the testing period is
562 estimated to be equal to 891.8 W m^{-2}.
563 The time evolutions of the ambient temperature, load temperature and global solar
564 irradiance measured during the tests of the panel and box cookers during different periods
565 on different days are depicted in Fig. 4.
566 The initial temperature of the load fluid in both tests is close to the respective ambient
567 outdoor air temperatures. At the end of each test, the temperature values of the testing
568 fluid are 146.0 ºC and 286 ºC, respectively, for the panel cooker and for the box cooker.
569 When testing the panel cooker, the average and maximum values of the wind velocity
570 were, respectively, 0.6 and 3.0 m s^{-1}. The wind velocity was not measured during the box
571 cooker test. However, its influence on the performance of this particular design is
572 expected to be almost negligible, because it is thermally well insulated and the funnel
573 reflector provides good protection of the glass cover against the wind.
574 The average values of the solar irradiance and ambient air temperature for the panel
575 cooker tested on an autumn day and for the box cooker tested on a summer day are listed
576 in Table 1, as well as the initial temperature of the load in each test. The thermal

577 capacitance of the system associated with the load alone [16] was estimated to be
578 Ω =5546 J ºC^{-1} for the panel cooker test and Ω=6581 J ºC^{-1} for the box cooker test.
579

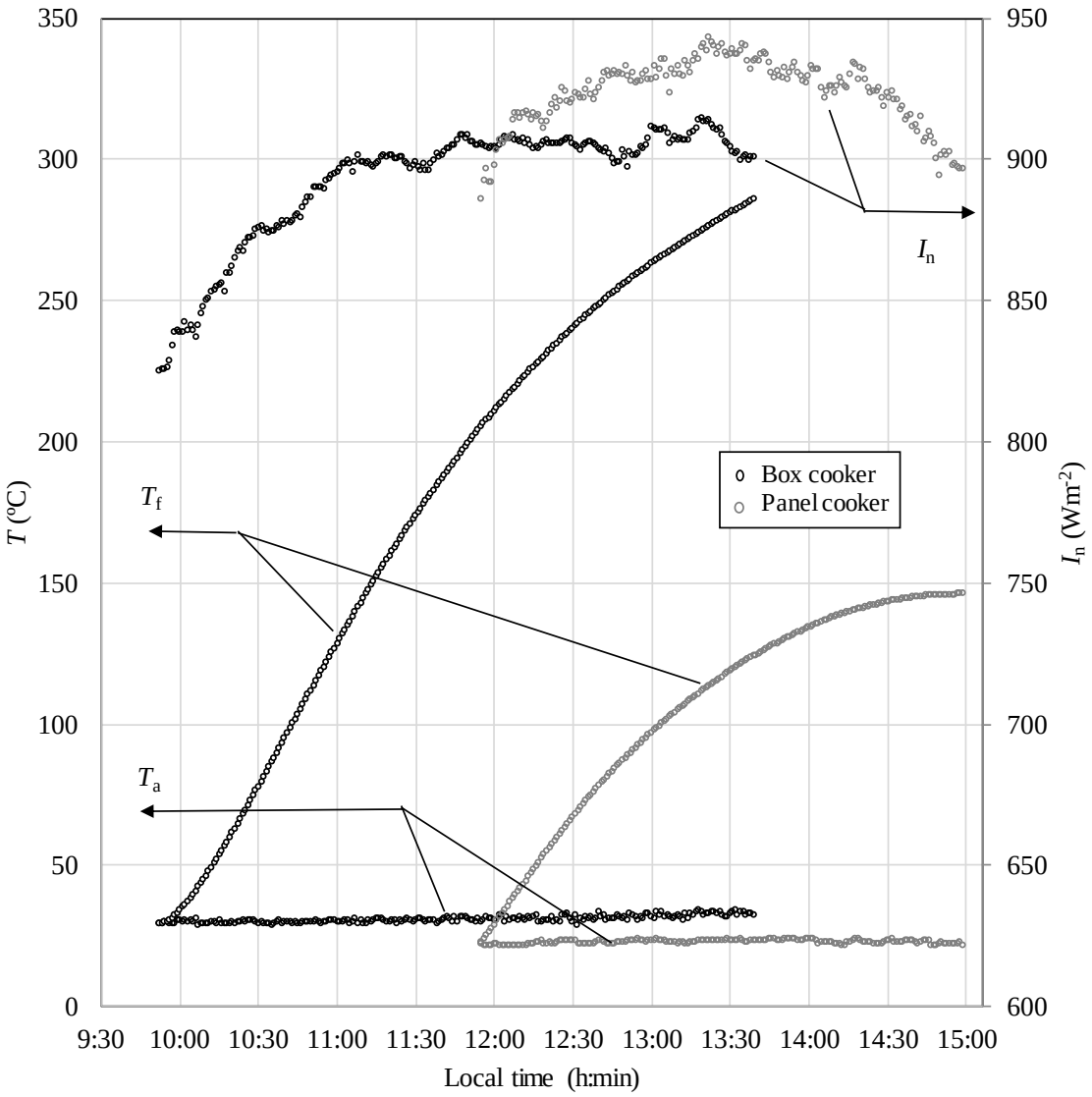

580

581 Fig. 4. Data from selected tests of the box cooker on 1 July 2016 and of the panel
582 cooker on 11 November 2020.

583

584 Table 1- Values of measured parameters during the test of panel and box cookers.

Parameter	Panel cooker	Box cooker

Average air temperature $\bar{T}_a$ (ºC)	22.7	30.8
Average solar irradiance $\bar{I}_n$ (W m^{-2})	913	891.8
Initial load temperature $T_{f,0}$ (ºC)	22.8	29.1

585

586 **3.2 Performance parameters of panel and box cookers**

587 The parameters of the first and the second order exponential polynomials expressed,
588 respectively, by Eq. (8) and Eq. (22), were determined for load temperature evolutions of
589 both cookers shown in Figs. 2 and 3. Microsoft Excel Solver was used for this purpose.
590 The achieved values are listed in Table 2 as well as the root mean square error.

591

592 Table 2- Parameters of the first and second order exponential polynomials.

Parameters of first order exponential polynomial (Eq. (8))					
	t_1 (s)	$c_{1,0}$ (ºC)	$c_{1,1}$ (ºC)	--	*RMSE* (ºC)
Panel cooker	5189.9	167.67	-149.01	--	1.32
Box cooker	11543	414.91	-403.81	--	3.85
Parameters of second order exponential polynomial (Eq. (22))					
	t_2 (s)	$c_{2,0}$ (ºC)	$c_{2,1}$ (ºC)	$c_{2,2}$	*RMSE* (ºC)
Panel cooker	3672.7	157.81	-196.14	61.29	0.63
Box cooker	5483.0	326.59	-524.55	224.21	0.48

593

594 Using the data from Table 2, the linear regression (curve 1) corresponding to the first
595 order exponential polynomial and the non-linear regression (curve 2) corresponding to
596 the second order polynomial, displayed qualitatively in Fig. 1b), are depicted in terms of
597 efficiency in Fig. 5 for the panel cooker and in Fig. 6 for the box cooker. The plots
598 obtained by using the experimental data in Eq. (2) are also depicted in Figs. 5 and 6. Table
599 3 lists the values of the parameters associated with points H1, V1 and R1 of curve 1 and

600 with points H2, V2, R2 and C2 of curve 2, shown in Fig. 1b). The same Table 3 also lists
601 the coordinates of similar points for the experimental plots.
602 The experimental plot of the panel cooker depicted in Fig. 5 shows that, during most of
603 the heating process, the linear fit associated with curve 1 is good. At the end of the test, a
604 small deviation is observed between the experimental plot and curves 1 and 2.
605 As mentioned before, the non-linear trend of the experimental plot in the final period
606 could be explained by the expected changes in the thermal resistances associated with the
607 heat transfer being lost by convection and by radiation. In the present case, this was not
608 the main reason because the temperature of the load was not very high. The main reason
609 is that a continuous reduction in the optical efficiency, seen at the end of the test, resulted
610 from a significant continuous increase in the angle of incidence during the final part of
611 the test. If the test of the panel cooker was conducted with perfect tracking in both axes,
612 the optical efficiency would be almost constant, and the experimental plot would be closer
613 than the two curves 1 and 2. The deviation between curve 1 and curve 2 is relatively small
614 at the end of the test. The experimental plot presents points for the whole specific
615 temperature difference range because the test ended when the load was very close to the
616 maximum temperature. In the case of the box cooker, this not occur because the test ended
617 far below the maximum expected load temperature. From the value of χ_{H2} listed in Table
618 3 for the box cooker obtained with the curve, the maximum load temperature is estimated
619 to be around 326 ºC, which lies well above normal cooking temperatures, and would be
620 potentially dangerous. The points determined directly with experimental data in the last
621 part for the panel cooker are perhaps not very accurate due to the error in estimating the
622 finite derivative with experimental measured data in this period of the test, in which the
623 rate of temperature increase is too slow. In the case of the panel cooker, it is observed that
624 point R2 is on the right side but closer to point C2.

In the case of the box cooker, by contrast, R2 is on the left and more distant from point C2. As can be seen in Fig. 6, it is clear that curve 1 is not credible because its linear trend is not consistent with accepted physics. The difference between the abscissa χ_{H1} of the linear trend and the value of the abscissa χ_{H2} is estimated to be around 30%, which is a large deviation. So, the determination of the cooker opto-thermal ratio based on curve 1 is questionable for some types of cooker. The results of this study show that the procedure based on curve 2 is more appropriate for estimating the cooker opto-thermal ratio, the power of the cooker and its efficiency. Cooker designs with point C2 positioned far from the beginning of the test should also be tested by inserting the load after a suitable pre-heating period. This is a research topic beyond the scope of the present study, but it is an interesting aspect that should also be investigated by reporting the performance of a cooker using different pre-heating periods.

It would also be important to test other designs of solar cooker, such as parabolic cookers, to investigate whether the slope of the performance curve changes during the final period for cases with maximum load temperatures between 150 ºC and 220 ºC, and the difference between curve 2 and the experimental data from such cooker designs.

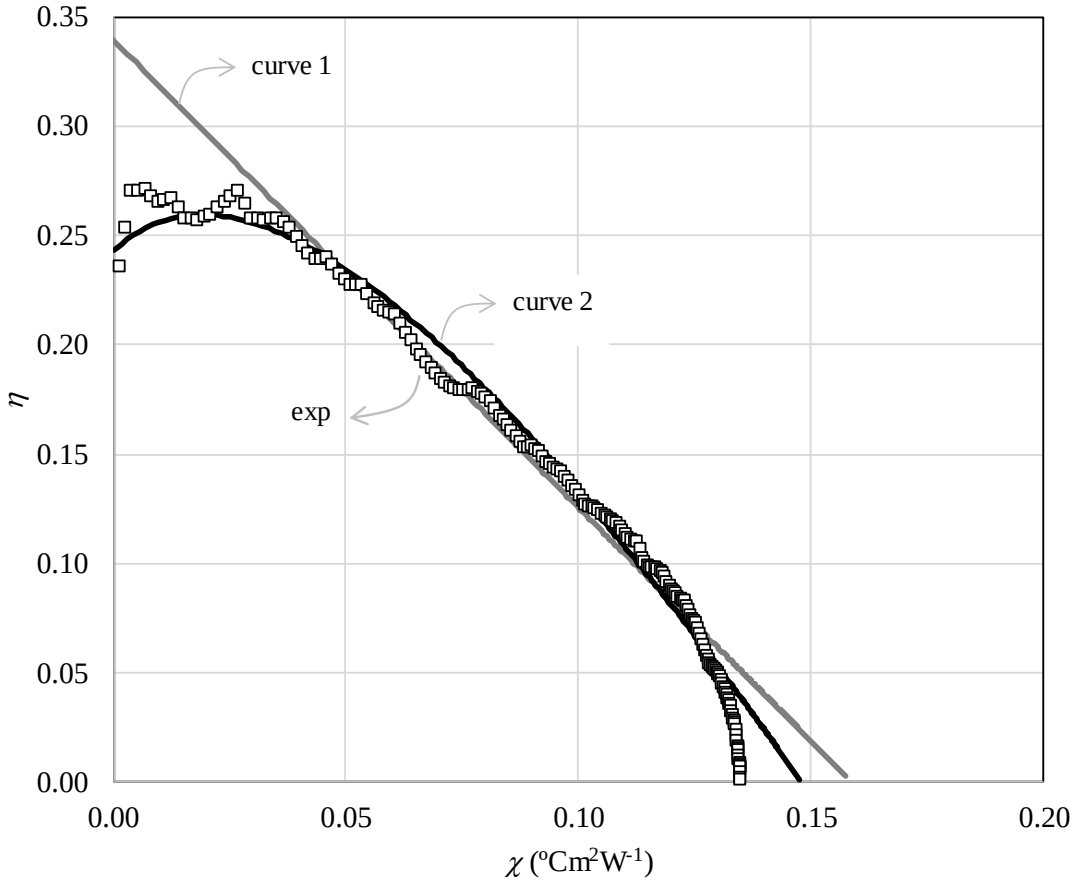

641

642 Fig. 5- Performance curves associated with the panel cooker test.

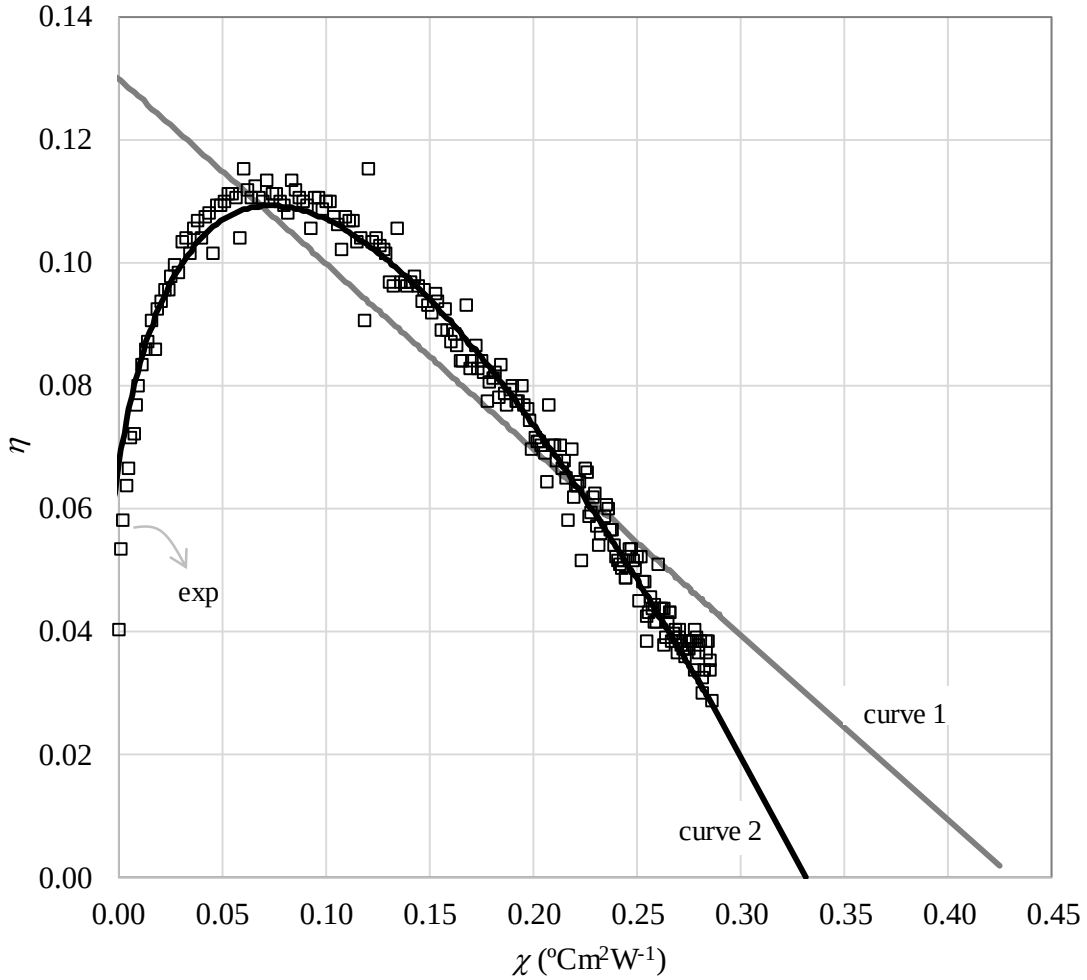

643

644 Fig. 6- Performance curves associated with the box cooker test.

645

646 Table 3- Performance parameters of at particular points of curve 2 and the corresponding

647 points of the experimental curve.

Points	V2		H2		R2		C2	
Cooker	χ_{V2}	η_{V2}	χ_{H2}	η_{H2}	χ_{R2}	η_{R2}	χ_{C2}	η_{C2}
Panel (curve 2	0.000	0.243	0.148	0.000	0.055	0.227	0.019	0.260
Panel (Exp.)	0.001	0.236	0.135	0.000	0.055	0.223	0.019	0.258
Box (curve 2)	-0.005	0.054	0.332	0.000	0.056	0.108	0.074	0.109
Box (Exp.)	0.000	0.040	--	--	0.056	0.111	0.074	0.111

648

649 **4. Conclusions**

In the present work, the first order exponential polynomial adopted in a previous work [16] and a new approach based on a second order exponential polynomial fit for the time evolution of two solar cookers, a panel and a box cooker, were evaluated. The mathematical formulation associated with both linear and non-linear performance curve approaches were presented in detail. The performance curves for each cooker were determined in terms of the relationship between the efficiency parameter and the specific temperature difference. The performance curves obtained with the first and second order exponential polynomials were compared with the curve determined directly from experimentally measured data. It was observed that the initial transient period due to warming up is properly described only by the performance curve derived from the second order exponential polynomial fit. The use of the linear regression, as recommended by the ASAE S580.1 Standard or derived from the first order exponential polynomial, cannot be considered useful for testing some designs of solar cooker, such as the box cooker considered here.

Reporting cooker performance based on a procedure supported only by fitting experimental data with a first order exponential polynomial seems to be good enough for a large number of solar cooker designs. However, it has some limitations: the initial period associated with the warming up of the cooker cannot be modelled with accuracy. Therefore, the authors of this study believe that the findings of the present investigation are highly valuable for updating the ASAE S580.1 Standard. In this context, instead of reporting the performance of the cooker in terms of standardised power at a temperature difference of 50 ºC between water and outdoor air temperature, the efficiency of the cooker should be reported for the following points: initial instant (point V2), when efficiency achieves its maximum value (point C2), standard reference point (point R2),

additional reference point close to water boiling condition and when load temperature achieves its maximum value (point H2).

For consolidation of the results of the new approach, a further research project is being planned by testing at the same time two units of a specific box cooker prototype where some modifications to the cooking chamber can be made. These modifications include: i) the replacement of a single glazed cover with a double glazed cover, ii) exchanging a thin metal sheet for the inner box with a thick metal sheet, and iii) the use of storage media with different weights and thicknesses of insulation material. The authors are confident that the novelty of the present work will motivate other research teams to investigate a universal procedure for testing and reporting the performance of different designs of solar cooker.

Acknowledgements

The authors would like to acknowledge Mr. Dave Oxford, of SLiCKsolarstove UK, for his valuable help in reviewing and revising the manuscript for grammar and syntax.

Credit authorship contribution statement

Xabier Apaolaza-Pagoaga: editing and writing-reviewing, investigation.

Gianluca Coccia: editing and writing-reviewing, investigation.

Celestino Rodrigues Ruivo: conceptualization, methodology, editing and writing-reviewing, formal analysis, supervision.

Antonio Carrillo-Andrés: editing and writing-reviewing.

References

[1] S. Nandwani, Design, construction and study of a hybrid solar food processor in the climate of Costa Rica, Renew. Energy 32 (2007) 427–441, https://doi.org/10.1016/j.renene.2006.01.019.

[2] A. Lecuona, J. Nogueira, R. Ventas, M. Rodríguez-Hidalgo M. Legrand, Solar cooker of the portable parabolic type incorporating heat storage based on PCM, Appl. Energy 111 (2013) 1136–1146, https://doi.org/10.1016/j.apenergy.2013.01.083.

[3] G. Coccia, G. Di Nicola, M. Pierantozzi, S. Tomassetti, A. Aquilanti, Design, manufacturing, and test of a high concentration ratio solar box cooker with multiple reflectors, Sol. Energy 155 (2017) 781–792, https://doi.org/10.1016/j.solener.2017.07.020.

[4] M. Collares-Pereira, A. Cavaco, A. Tavares, Figures of merit and their relevance in the context of a standard testing and performance comparison methods for solar box – Cookers, Sol. Energy 166 (2018) 21–27, https://doi.org/10.1016/j.solener.2018.03.040.

[5] I. Edmonds, Low-cost realisation of a high temperature solar cooker, Renew. Energy 121 (2018) 94–101, https://doi.org/10.1016/j.renene.2018.01.010.

[6] A.A. Sagade, S.K. Samdarshi, P.S. Panja, Enabling rating of intermediate temperature solar cookers using different working fluids as test loads and its validation through a design change, Sol. Energy 171 (2018) 354–365, https://doi.org/10.1016/j.solener.2018.06.088.

[7] S. Ebersviller, J. Jetter, Evaluation of performance of household solar cookers, Sol. Energy 208 (2020) 166–172, https://doi.org/10.1016/j.solener.2020.07.056.

[8] ASAE S580.1 NOV2013, Testing and reporting solar cooker performance, American Society of Agricultural Engineers, Michigan, USA, 2013. [19] ASAE S580.1

NOV2013, Testing and reporting solar cooker performance, American Society of Agricultural Engineers, Michigan, USA, 2013.

[9] A. Khallaf, M. Tawfik, A. El-Sebaii, A. Sagade, Mathematical modeling and experimental validation of the thermal performance of a novel design solar cooker, Sol. Energy 207 (2020) 40–50, https://doi.org/10.1016/j.solener.2020.06.069.

[10] A.A. Sagade, S.K. Samdarshi, P.-J. Lahkar, N.A. Sagade, Experimental determination of the thermal performance of a solar box cooker with modified cooking pot, Renew. Energy 150 (2020) 1001–1009, https://doi.org/10.1016/j.renene.2019.11.114.

[11] M.A. Tawfik, A. Sagade, R. Palma-Behnke, H. El-Shal, W. Allah, Solar cooker with tracking-type bottom reflector: An experimental thermal performance evaluation of a new design, Sol. Energy 220 (2021) 295–315, https://doi.org/10.1016/j.solener.2021.03.063.

[12] C. Ruivo, A. Carrillo-Andrés, X. Apaolaza-Pagoaga, Experimental determination of the standardised power of a solar funnel cooker for low sun elevations, Renew. Energy 170 (2021) 364–374, https://doi.org/10.1016/j.renene.2021.01.146.

[13] X. Apaolaza-Pagoaga, A. Sagade, C. Ruivo, A. Carrillo-Andrés, Performance of solar funnel cookers using intermediate temperature test load under low sun elevation, Sol. Energy 225 (2021) 978–1000, https://doi.org/10.1016/j.solener.2021.08.006.

[14] X. Apaolaza-Pagoaga, A. Carrillo-Andrés, C. Ruivo, New approach for analysing the effect of minor and major solar cooker design changes: Influence of height trivet on the power of a funnel cooker, Renew. Energy 179 (2021) 2071–2085, https://doi.org/10.1016/j.renene.2021.08.025.

745 [15] P.J. Lahkar, R.K. Bhamu, S.K. Samdarshi, Enabling inter-cooker thermal
746 performance comparison based on cooker opto–thermal ratio (COR), Appl. Energy,
747 99 (2012) 491–495, https://doi.org/10.1016/j.apenergy.2012.05.034.
748 [16] C. Ruivo, X. Apaolaza-Pagoaga, G. Di Nicola, A. Carrillo-Andrés, On the use of
749 experimental measured data to derive the linear regression usually adopted for
750 determining the performance parameters of a solar cooker, Renew. Energy 181 (2022)
751 105–115, https://doi.org/10.1016/j.renene.2021.09.047.
752 [17] P.A. Funk, Evaluating the international standard procedure for testing solar cookers
753 and reporting performance, Sol. Energy 68 (2000) 1–7, https://doi.org/10.1016/S0038-
754 092X(99)00059-6.
755 [18] G. Coccia, A. Aquilanti, S. Tomassetti, A. Ishibashi, G. Di Nicola, Design,
756 manufacture and test of a low-cost solar cooker with high-performance light-
757 concentrating lens, Sol. Energy 224 (2021) 1028–1039,
758 https://doi.org/10.1016/j.solener.2021.06.025.
759 [19] Solar Cookers International, https://www.solarcookers.org/resources/results
760 (Accessed 30 September 2021).
761 [20] V.P. Sethi, D.S. Pal, K. Sumathy, Performance evaluation and solar radiation capture
762 of optimally inclined box type solar cooker with parallelepiped cooking vessel design,
763 Energy Convers. Manage. 81 (2014) 231–241,
764 https://doi.org/10.1016/j.enconman.2014.02.041.
765 [21] Cookit, Solar cooking Wiki. https://solarcooking.fandom.com/wiki/CooKit.
766 (Accessed 6 October 2021).
767 [22] Hartmut Ehmler. https://solarcooking.fandom.com/wiki/Hartmut_Ehmler.
768 (Accessed 6 October 2021).
769 [23] Haines solar cookers. https://hainessolarcookers.com/. (Accessed 6 October 2021).

[24] A.A. El-Sebaii, A. Ibrahim, Experimental testing of a box-type solar cooker using the standard procedure of cooking power, Renew. Energy 30 (2005) 1861–1871, https://doi.org/10.1016/j.renene.2005.01.007.

[25] J.A. Duffie, W.A. Beckman, Solar Engineering of Thermal Processes, fourth ed., Willey, 2013.

[26] G. Coccia, G. Di Nicola, M. Pierantozzi, S. Tomassetti, A. Aquilanti, Corrigendum to “Design, manufacturing, and test of a high concentration ratio solar box cooker with multiple reflectors” [Sol. Energy 155 (2017) 781–792], Sol. Energy 234 (2022) 400-404, https://doi.org/10.1016/j.solener.2021.11.038.